

Article

Wear-Resistant Elastomeric Composites Based on Unvulcanized Rubber Compound and Recycled Polytetrafluoroethylene

Oksana Ayurova ^{1,*}, Vasiliy Kornopoltsev ¹, Andrey Khagleev ^{2,3} , Roman Kurbatov ¹,
Undrakh Mishigdorzhijn ² , Afanasiy Dyakonov ⁴ and Dmitriy Mogonov ³

¹ Baikal Institute of Nature Management of the Siberian Branch of the Russian Academy of Sciences, Sakhyanovoy Str. 6, 670047 Ulan-Ude, Russia; kompo@mail.ru (V.K.); kurbatov@binm.ru (R.K.)

² Institute of Physical Materials Science of the Siberian Branch of the Russian Academy of Sciences, Sakhyanovoy Str. 6, 670047 Ulan-Ude, Russia; khagleev@yandex.ru (A.K.); mishigdorzh@gmail.com (U.M.)

³ Faculty of Civil Engineering, East Siberia State University of Technology and Management, Klyuchevskaya 40b, 670013 Ulan-Ude, Russia; dmog@binm.ru

⁴ Laboratory of Polymer Nanocomposites Technologies, North-Eastern Federal University in Yakutsk, Belinskogo Str. 58, 677000 Yakutsk, Russia; afonya71185@mail.ru

* Correspondence: chem88@mail.ru

Abstract: Advancements in industrial machinery and manufacturing equipment require more reliable and efficient polymer tribo-systems which operate in conditions associated with increasing machine speeds and a lack of cooling oil. The goal of the current research is to improve the tribological properties of elastomeric composites by adding a solid lubricant filler in the form of ultrafine polytetrafluoroethylene (PTFE) with the chemical formula $[C_2F_4]_n$ and recycled polytetrafluoroethylene (r-PTFE) powders. PTFE waste is recycled mechanically by abrasion. The elastomeric composites are prepared by mixing a nitrile butadiene rubber with a phenol-formaldehyde resin and PTFE powders in an extruder followed by rolling. The deformation-strength and tribological tests of r-PTFE elastomeric composites are conducted in comparison with the ultrafine PTFE composites. The latter is based on products of waste fluoropolymer processing using a radiation method. The deformation-strength test shows that the introduction of ultrafine PTFE and r-PTFE powder to the composite leads to a decrease in strength and elongation at break, which is associated with the poor compatibility of additives and the elastomeric matrix. The friction test indicates a decrease in the coefficient of friction of the composite material. It is determined that the 15 wt.% filler added in the elastomeric matrix leads to a reduction in the wear rate by 20%. The results obtained show the possibility of using ultrafine PTFE powder and r-PTFE for creating elastomeric composites with increased tribological properties. These research results are beneficial for rubber products used in many industries, mainly in mechanical engineering.

Keywords: unvulcanized rubber compound; phenol formaldehyde resin; recycled polytetrafluoroethylene; elastomeric composite; wear resistance



Citation: Ayurova, O.; Kornopoltsev, V.; Khagleev, A.; Kurbatov, R.; Mishigdorzhijn, U.; Dyakonov, A.; Mogonov, D. Wear-Resistant Elastomeric Composites Based on Unvulcanized Rubber Compound and Recycled Polytetrafluoroethylene.

Lubricants **2024**, *12*, 29. <https://doi.org/10.3390/lubricants12020029>

Received: 21 November 2023

Revised: 7 January 2024

Accepted: 10 January 2024

Published: 24 January 2024



Copyright: © 2024 by the authors. Licensee MDPI, Basel, Switzerland. This article is an open access article distributed under the terms and conditions of the Creative Commons Attribution (CC BY) license (<https://creativecommons.org/licenses/by/4.0/>).

1. Introduction

Despite the fact that rubber products made on the basis of nitrile butadiene rubber have a whole range of excellent properties, including high tensile strength and ductility, relative elongation, tensile and abrasion resistance, and excellent oil and gasoline resistance, this material also has some flaws. Tightening operating conditions associated with increasing machine speeds and a lack of cooling oil leads to the fact that rubber elements can only operate at temperatures up to +150 °C. In the case that the operating temperature increases above this value, the structuring and then the destruction of rubber occurs, i.e., heated rubber becomes hard and brittle. Exposure to low temperatures also has a negative effect on rubber products manufactured using nitrile butadiene rubber. The optimal operating temperature for them is considered to be no lower than −35 °C. It is known that the

addition of materials to elastomers that have higher mechanical properties and resistance to aggressive environments over a wide temperature range can significantly increase their impact strength characteristics [1–7]. The advantage of such composites is the ability to combine in one material the properties of significantly different components, for example, rubber and thermoplastic or rubber and thermoset [8–10]. A high complex of physical and mechanical properties of such composites is ensured by the uniform distribution of filler particles in the elastomeric matrix, as well as the chemical interaction between the components of the polymer mixture during the mixing process. In early works [9–14] in this direction, modifications of polystyrene and epoxy resin were used, including thermosets such as phenol-aldehyde resins. Zhang et al. [15] show that treating reinforcing fiber by resorcinol–formaldehyde resin leads to better adhesion to natural rubber. The interfacial strength of the resulting composites reached 10 MPa. In a previous study, we reported on the modification of nitrile rubber by phenol–formaldehyde resin [16]. The interaction of these materials results in semi-interpenetrating polymer networks' formation by structuring the thermoset on a linear polymer matrix. The components of such a mixture are inseparable due to the mechanical interweaving of the chains. In addition, chemical interaction between the methylol group of the resin and the nitrile fragment of the rubber can lead to a noticeable increase in the level of strength. Complete structuring is not observed, which is explained by the difficulty of diffusion due to a decrease in the segmental mobility of the interacting polymers. The inclusion of 15 wt.% resin in nitrile butadiene rubber leads to the production of materials with excellent deformation-strength properties ($\delta p = 10\text{--}15$ MPa, $\epsilon p = 150\text{--}270\%$, Shore hardness 76–93), which allows their use in hydraulic systems with increased pressure of working media.

For the wider use of rubber products, it is necessary to enhance the mechanical and tribological properties by adding antifriction fillers. The wear resistance and low friction properties of polymers can generally be improved by incorporating carbon; glass and steel fibers; and solid lubricants such as graphite, polytetrafluoroethylene (PTFE), molybdenum disulfide MoS_2 , etc. [17]. It is known that polytetrafluoroethylene is one of the best anti-friction materials, which characterized by a low coefficient of friction, high heat resistance, and performance in a wide temperature range from -269 to $+260$ °C [18]. A feature that enhances the usefulness of PTFE as a solid lubricant is the fact that it easily forms chemically stable transfer films on the opposing surface even at low pressures of only a few kPa. The friction surface consists of PTFE-PTFE contacts when forming a transfer film on the opposite surface, providing low friction. A number of studies show the application of PTFE as an internal solid lubricant for some polymers and demonstrate that the friction and wear-resistant properties of polymer matrices filled with PTFE are increased [7,17–25]. The high molecular weight and chemically inert surface of PTFE limit its use as an effective filler in polymer matrices, including elastomeric ones. The low surface energy of PTFE causes poor wetting and adhesion, which makes it difficult to uniformly disperse and chemically bond PTFE powder to rubber [23–25]. Special compounding processes have been developed to reduce the fibrillation effect and facilitate the dispersion of high-molecular-weight PTFE in elastomers. Methods for the surface modification of PTFE powder to improve compatibility with hydrocarbon elastomers and reduce agglomeration have also been reported [22,24–26]. It is known that high-energy gamma radiation and electron beam radiation affect the physical and mechanical properties of PTFE [27–30]. For instance, radiation-treated PTFE exhibits a better reinforcing effect than non-irradiated PTFE in polar systems [23]. Khan et al. [24,25] and Cao et al. [26] report that high-energy irradiation reduces the energy required to produce PTFE powder from its waste and results in a powder that does not agglomerate. Portnyagina et al. [31] show that the introduction of ultrafine polytetrafluoroethylene into propylene oxide rubber leads to a decrease in the coefficient of friction and an improvement in the wear resistance of the material by 21%. In addition, elastomeric composites containing 50 phr ultrafine PTFE perform stably under wear conditions over a wide range of loads and sliding speeds at a temperature of -25 °C [31].

The global consumption of polytetrafluoroethylene in various industries increases by 5–8% annually, which is due to its unique properties: high chemical and thermal resistance, good dielectric properties, and a low coefficient of friction. At the same time, a large amount of waste accumulates during the fabrication of PTFE products, which leads to environmental and economic problems [32,33]. In this regard, the issue of the polymer waste processing into commercial products or raw materials for further reuse becomes urgent.

The current research considers the novel approach to PTFE composites' production with enhanced tribological properties by using recycled PTFE waste. Hence, the goal of the work is to improve the tribological properties of elastomeric composites by introducing recycled PTFE. The influence of the PTFE waste recycling method on the properties and structure of recycled PTFE is assessed, and the properties of elastomeric composites are investigated. It should be noted that the approaches we use to obtain elastomeric composites are adapted to waste-free technology based on the processing and use of polymer waste, which leads to a reduction in environmental stress [34–38].

2. Materials and Methods

A polymer–polymer mixture based on an industrial unvulcanized rubber compound (URC) and phenol–formaldehyde resin (PhFR) was used as an elastomeric matrix.

Commercial URC of 3826 grade according to Technical Specifications No. 2512-046-00152081-2003 is intended for the manufacture of rubber products operating in contact with oils and fuels, such as rings, cuffs, technical plates, etc. Its operating temperature range is from -20 to $+100$ °C. Shore A hardness is 50–75. The base component of the URC of 3826 grade is nitrile butadiene synthetic rubber type BNKS-40 according to Technical Specifications No. 38.30313-2006.

Phenol–formaldehyde resin of SF-010A grade (resin type is Novolaks) is an irregularly shaped piece of dark yellow color, produced by Uralchimplast LLC (Nizhny Tagil, Russia) according to State Standard No. 18694-80 [39]. Phenol–formaldehyde resin was melted at 80 – 90 °C, and 8–12% of dinitrile was introduced. The mixture was stirred until the hardener was completely dissolved. After its cooling down to room temperature, it was ground into a powder.

The polymer–polymer mixture was prepared by mixing URC with prepared PhFR on a screw extruder in a ratio of 85 wt.% rubber and 15 wt.% resin, followed by rolling. At first, URC in the form of a strip was placed in an extruder and spun. The obtained prepack product was passed through rollers to produce a sheet of 1 mm thick. Then, PhFR powder was evenly distributed onto the rolled rubber sheet, and the sheet was rolled lengthwise and passed through rollers. The resulting polymer–polymer composition was passed through an extruder and then again through rollers for the more uniform distribution of PhFR particles in URC. The cycle was repeated several times until a uniform polymer–polymer mixture was obtained. Elastomeric composites were prepared by mixing the URC/PhFR polymer–polymer mixture and recycled polytetrafluoroethylene (r-PTFE, TOMFLON™) powder in an extruder followed by rolling according to the scheme depicted on Figure 1. Recycled PTFE powder was evenly distributed onto a rolled sheet of the URC/PhFR mixture. Then, the sheet was twisted and passed through rollers and the extruder. Operations using rollers and an extruder were repeated 5 times. The content of recycled polytetrafluoroethylene in the composite was 10, 15, 20, and 30 wt.%.

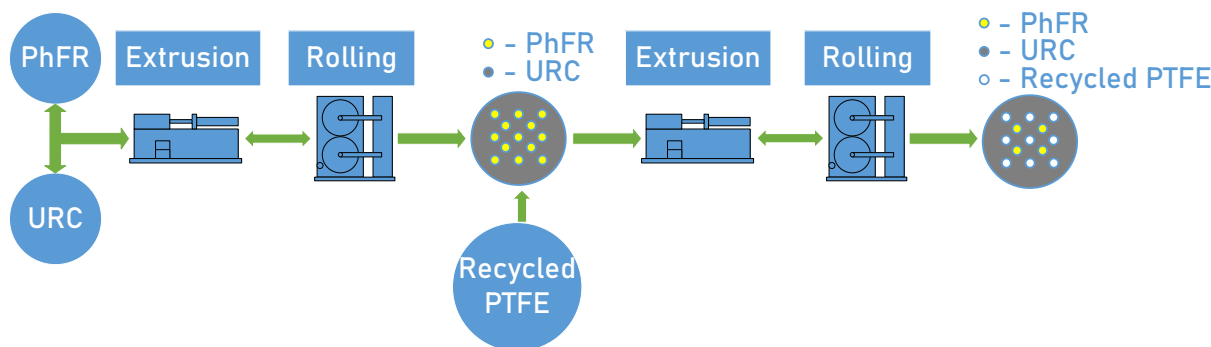


Figure 1. The procedure of elastomeric composite fabrication.

The co-rotating extruder with screw thread and screw feed with 60 rpm was used for the experiments. The size of the extruder working area (L/D) was 25 cm × 15 cm.

Ultrafine polytetrafluoroethylene of the TOMFLON™ trademark is a loose friable white powder with a particle size of ~5 μm (Technical Specifications No. 2213-001-12435252-03) produced by radiation in Fluoropolymer Technologies LLC (Tomsk, Russia). This method of processing PTFE waste is a combinational one, combining radiation and mechanical processing. Radiation treatment is carried out by accelerated electrons and leads to the accumulation of defects, which in turn initiate the appearance of micro- and macrocracks in the polymer. During the subsequent mechanical processing of the material in jet mills, the particles are destroyed along these defects. As a result, ribbon-shaped particles are formed whose molecular structure completely corresponds to the structure of industrial samples of polytetrafluoroethylene [38].

Recycled polytetrafluoroethylene (r-PTFE) was produced by mechanically grinding waste polymer by attrition in a designed and manufactured plant [34]. The particle sizes of the powder obtained by this method have a wide scatter and are in the range of 5–100 μm.

Micrographs of the fluoropolymer powders were obtained using an optical microscope Altami MET 2C with 5 MP camera and Altami Studio program. Samples of r-PTFE and TOMFLON™ powders were dispersed by ultrasonication in an GA008G ultrasonic bath (40 kHz, 60 W) for 2 min in ethyl alcohol and then placed on a glass substrate.

X-ray diffraction data of the samples were obtained at room temperature on a D8 ADVANCE Bruker AXS powder diffractometer with a Vantec-1 detector (CuK α radiation; shooting interval $2\theta = 10\text{--}70^\circ$; scanning step— 0.02076°). The processing of experimental data using full-profile analysis methods and the calculation of the degree of crystallinity were performed using the TOPAS 4.2 software package [40]. The profile analysis procedure is based on modeling an experimental X-ray pattern by the sum of approximating functions for the background and individual diffraction maxima [41]. A 1st-degree Chebyshev polynomial was used to model the XRD pattern background. The total integrated intensity of all observed reflections, which were described by the Split-PearsonVII analytical functions, was taken as the crystalline component of PTFE. Split-PseudoVoigt analytical functions were used to model the amorphous contribution [40]. The refinement of variation parameters by nonlinear OLS was stable and resulted in low R_{wp} factors. The degree of crystallinity of the sample was calculated automatically in Topas 4.2 software using the formula [42] $\text{degree_of_crystallinity} = 100 \times \text{crystalline_area} / (\text{crystalline_area} + \text{amorphous_area})$, where $\text{degree_of_crystallinity}$ is the degree of crystallinity, crystalline_area is the total integral area of all peaks assigned to the crystalline component, and amorphous_area is the total area reflexes attributed to amorphous phases. Reflection areas are calculated automatically, taking into account the necessary corrections, e.g., Lorentz polarization.

Thermographic studies were carried out on a synchronous thermal analyzer STA 449C Netzsch at a temperature rise rate of $5^\circ/\text{min}$ in an air atmosphere, in corundum crucibles. The flow of the main gas N_2/O_2 was 50 mL/min, and the protective gas N_2/O_2 was 20 mL/min. The sample weight varied from 7 to 50 mg.

Morphological studies and local elemental analyses were carried out using scanning electron microscopy on a high-resolution microscope JSM-7800F Jeol with a mounted energy-dispersive microanalysis system X-MAX-20 Oxford Instruments in the laboratory of Technology of polymer nanocomposites of the North-Eastern Federal University in Yakutsk (Yakutsk, Russia). Sample preparation for studying the structure in the bulk of the samples was carried out using the brittle cleavage method by cooling in liquid nitrogen. Carbon was used to create a conductive layer on the surface of the samples.

Relative elongation and tensile strength were determined according to State Standard No. 11262-80 [43] on an INSTRON 3367 testing machine at room temperature and a moving speed of movable grips of 200 mm/min on standard blades. The number of samples per test was five. The tribological parameters (friction coefficient and wear rate) of the elastomeric composites were determined using an SMT-1 friction machine according to the following scheme: rotating shaft–fixed liner during friction without lubricants. The sliding speed was 0.85 m/s, the load was 5 kg, and the duration of the test was 3 h. For each material, five samples were used. A bushing made of carbon steel 45 (the analog to AISI 1045 steel) with a diffusion-hardened surface after boriding (2100 HV100), polished to $R_a < 0.01 \mu\text{m}$, was used as a counter-body. The chemical composition of AISI 1045 steel is given in Table 1. The relative wear rate of elastomeric composites was determined as the weight loss of the sample by the time of abrasion (mg/h). The weight loss of the samples was measured on an AGN-200 analytical balance every 10–15 min with an accuracy of $\pm 2 \times 10^{-3} \text{ g}$.

Table 1. The chemical composition AISI 1045 steel, wt.%.

Element	C	Mn	P	S	Fe
Content	0.42–0.5	0.6–0.9	up to 0.04	up to 0.05	98.51–98.98

3. Results

Figure 2 shows microimages of recycled r-PTFE and TOMFLON™ powders. The particle size of r-PTFE ranges from 5 to 180 μm (Figure 2a). TOMFLON™ is a powder that is more uniform in dispersion, the particles of which have a size of $\sim 5\text{--}10 \mu\text{m}$ (Figure 2b).

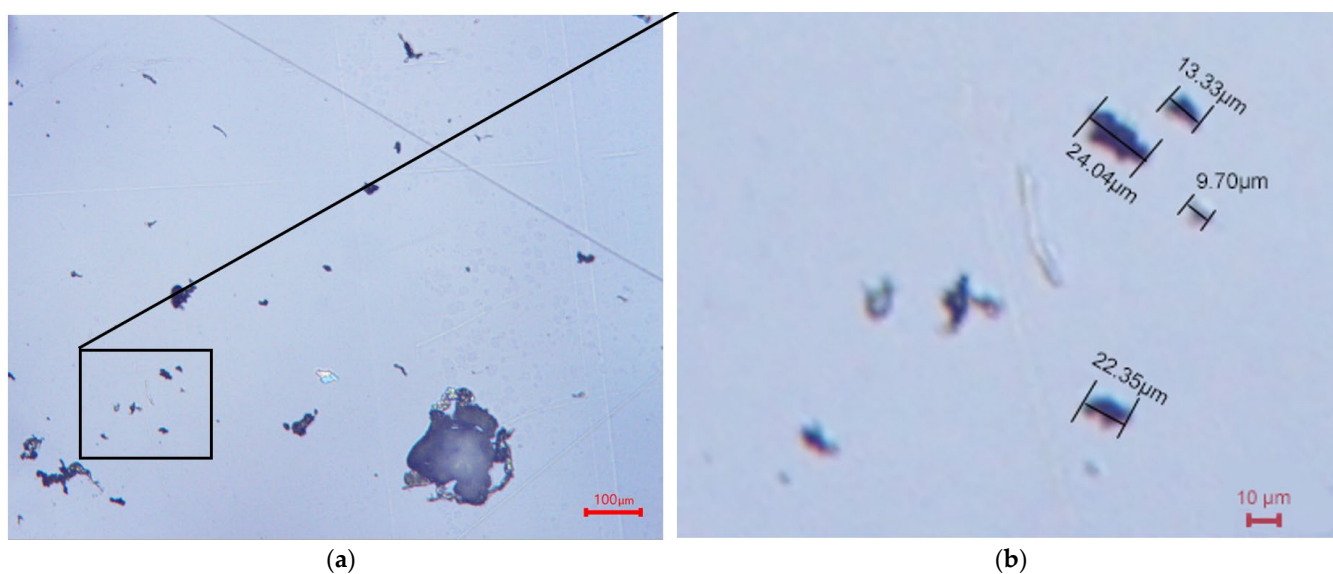


Figure 2. Cont.

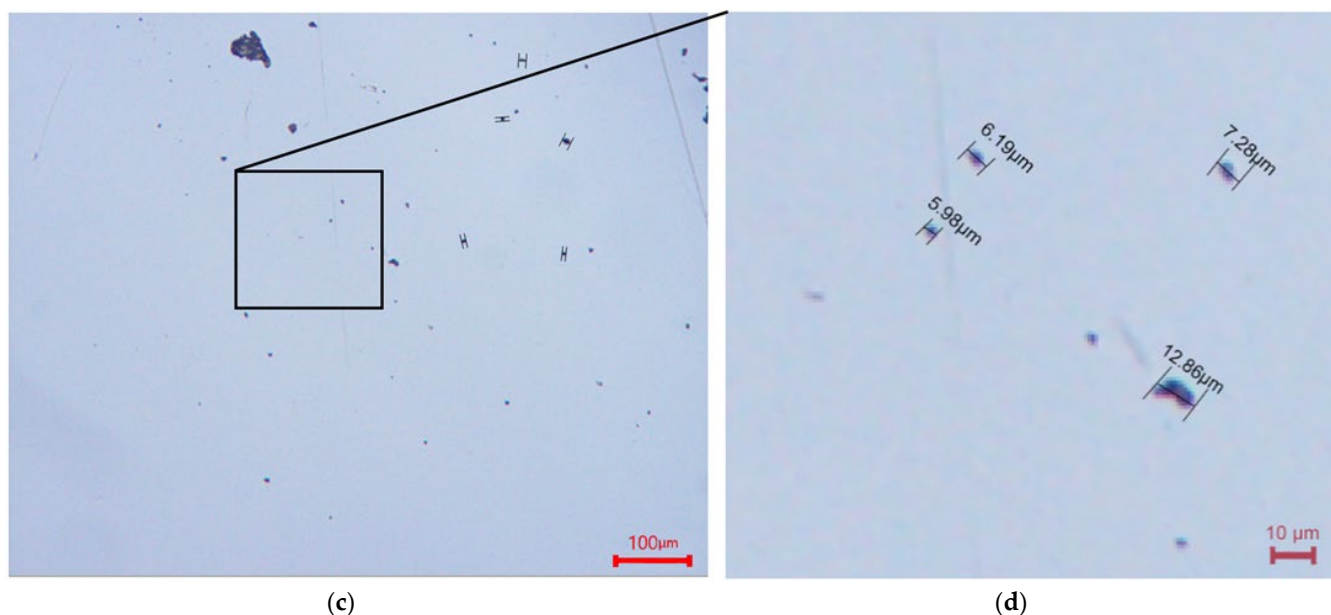


Figure 2. Microphotographs of PTFE powders: (a,b) r-PTFE; (c,d) TOMFLON™.

The XRD patterns show the most intense peak at 2θ 18° , small peaks in the region of 2θ 30 – 70° characteristic of the crystalline phase of polytetrafluoroethylene, and a halo for the amorphous phase in the region of 15 – 17° and 30 – 50° (Figure 3). All samples had a clear match with card 00-047-2217 of the ICDD database (PDF-2).

For all samples, a three-phase structure is observed: a crystalline phase and two amorphous components. The first amorphous phase (I), characterized by a diffuse maximum in the region 2θ around 16 – 17° , is the “ordinary” amorphous phase of the polymer, consisting of entangled chains of macromolecules, while another amorphous phase (II), observed at diffraction angles 2θ 30 – 50° , is a low-molecular amorphous formation with a molecular structure different from PTFE chains. The degree of crystallinity of the samples was determined as the ratio of the integral intensity of the crystalline reflection to the total intensity of this reflection and diffuse scattering located in the same region of diffraction angles [44–46]. For instance, Figure 4a presents the results of a profile analysis of WPTFE: experimental, calculated and difference X-ray diffraction patterns, as well as profiles of all reflections attributed to both the crystalline and amorphous components of the sample. The amorphous components of the polymer were taken to be the maximum of a diffuse nature, localized in the region 2θ around 16 – 17.5° , as well as a “powerful” amorphous halo with 2θ 38 – 40° (Figure 4b) [44–46]. Figure 4c shows the procedure for profile analysis based on modeling an experimental X-ray diffraction pattern by the sum of approximating functions for the background and individual diffraction maxima [41].

Table 2 presents the results of the profile analysis for all studied samples. Based on the data obtained, the quantitative ratios of the crystalline and amorphous phases I and II of WPTFE and processed PTFE powders were calculated, as well as the degree of crystallinity of the samples depending on the processing technology (Table 3).

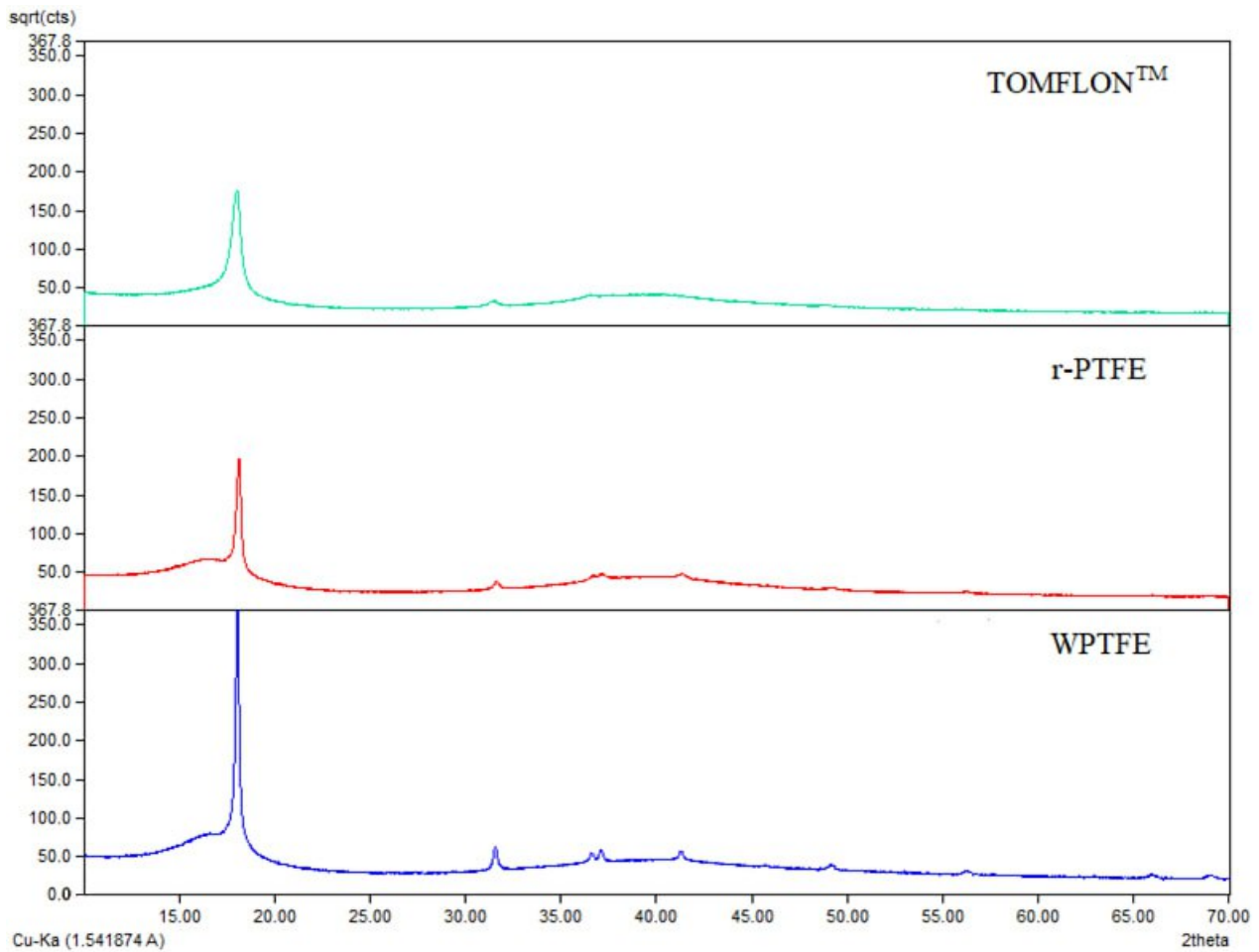
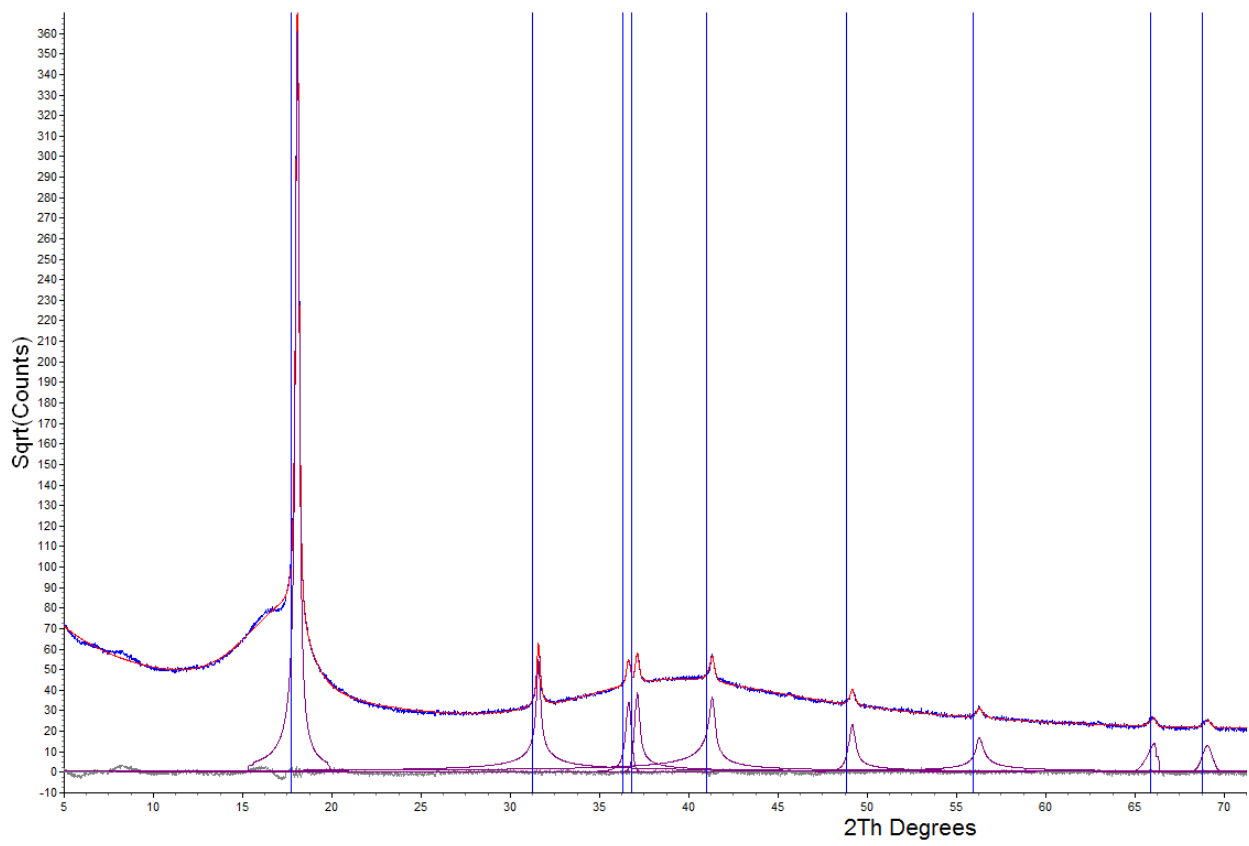


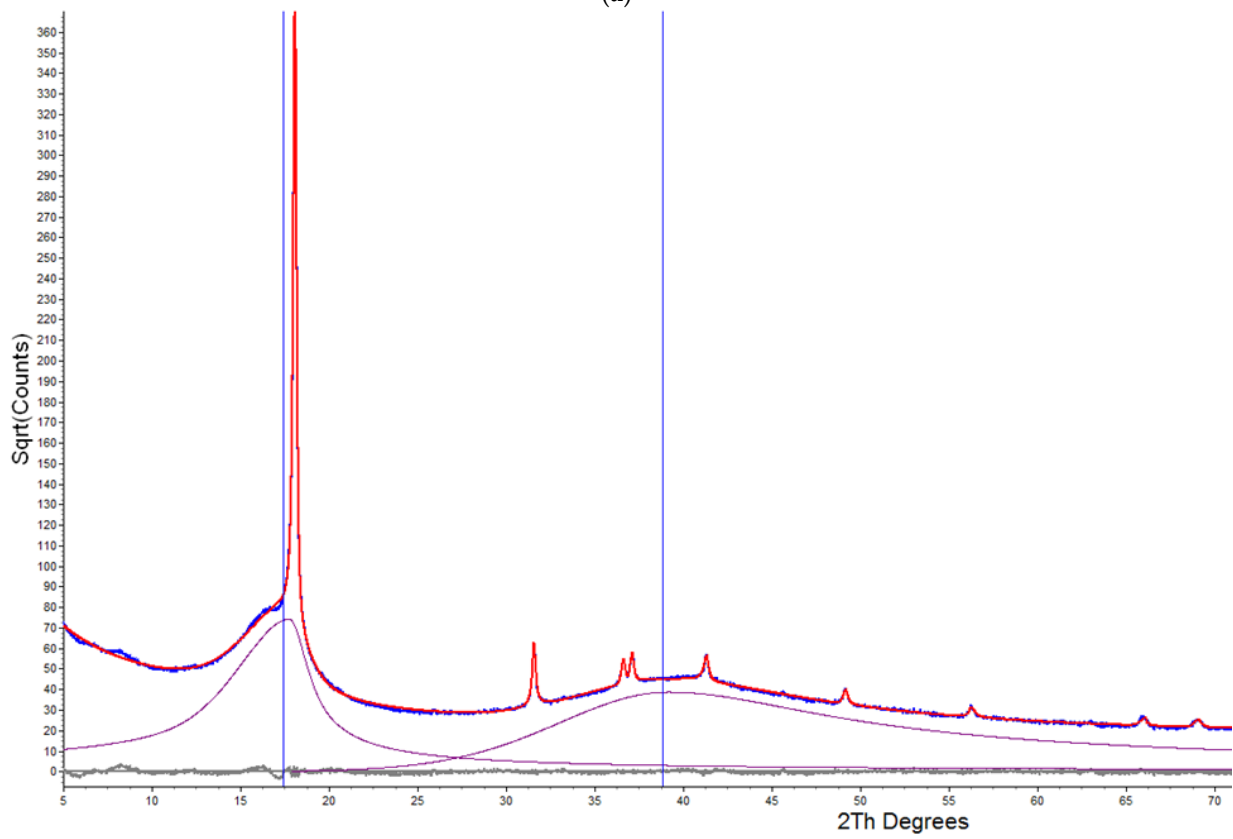
Figure 3. XRD patterns of the studied fluoropolymers.

Table 2. Results of profile analysis for all studied samples.

Sample	Phase	Reflection Positions by 2θ , °	Integral Peak Area	R_{wp}
WPTFE	Crystalline	17.7°; 31.2°; 36.3°; 36.8°; 41.0°; 48.9°; 55.9°; 65.9°; 68.8°	30,571.2152	4.079
	Amorphous I	17.4°	26,022.4045	
	Amorphous II	38.8°	27,561.4415	
r-PTFE	Crystalline	18.2°; 31.7°; 37.2°; 37.7°; 41.4°	37,831.0084	3.317
	Amorphous I	16.7°	19,139.5714	
	Amorphous II	40.1°	2274.41598	
TOMFLON™	Crystalline	18.1°; 31.6°; 36.6°; 40.4°	22,596.3958	6.069
	Amorphous I	17.3°	5457.07316	
	Amorphous II	38.2°	21,008.7386	



(a)



(b)

Figure 4. Cont.

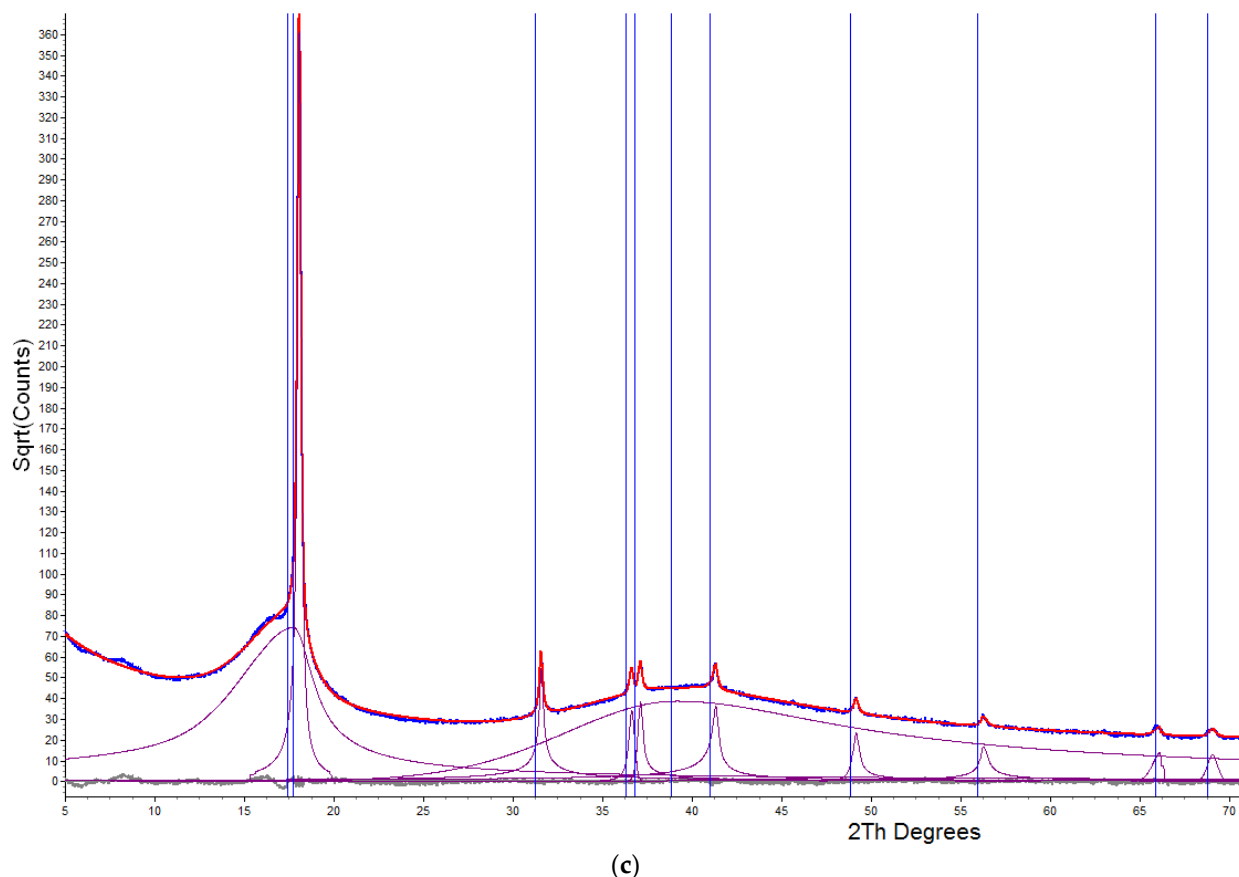


Figure 4. XRD patterns: (a) modeling of the peaks of the crystalline phase for the WPTFE sample; (b) modeling of halo of amorphous phases; (c) modeling of the entire radiograph, where blue line is experimental X-ray diffraction pattern indicated, red line is calculated radiograph indicated, gray line is difference radiograph, and lilac line is profiles of all reflections, assigned to both the crystalline component of the sample and the amorphous one.

Table 3. Phase composition and degree of crystallinity of the studied fluoropolymer samples.

No	Sample	Phase Composition, %			* Degree of Crystallinity, %
		Crystalline Phase	Amorphous Phase I	Amorphous Phase II	
1	WPTFE	36.3	30.9	32.8	54.0
2	r-PTFE	64.0	32.3	3.7	66.5
3	TOMFLON™	43.0	10.1	46.9	81.0

* The degree of crystallinity was calculated as the ratio of the fraction of the crystalline phase to the fractions of the crystalline and amorphous phase I.

The analysis of the data presented shows that the content of amorphous phase II for all fluoropolymers ranges from 3 to 50%. The TOMFLON™ sample has a significantly higher degree of crystallinity compared to the r-PTFE sample, which may be due to the virtually defect-free formation of polymer crystallites during irradiation with accelerated electrons followed by mechanical processing. When PTFE is irradiated, the rupture of macromolecular chains occurs predominantly in the amorphous region with the formation of shorter macromolecular chains. The increase in crystallinity upon irradiation can be explained by increased cross-linking at certain irradiation doses. The possible radiation rupture of the macromolecular chain, which causes the mobility of the resulting molecular fragments of the polymer, leads to the removal of residual stress in the amorphous region and a decrease in the likelihood of the entanglement of macromolecular chains with the formation of additional small crystallites [27]. Higher crystallinity (81%) is characteristic of

the sample with a lower molecular weight (TOMFLONTM), which is consistent with the results of TG and DSC (Figure 5). This indicates that during the radiation processing of PTFE, the polymer chain is broken [29].

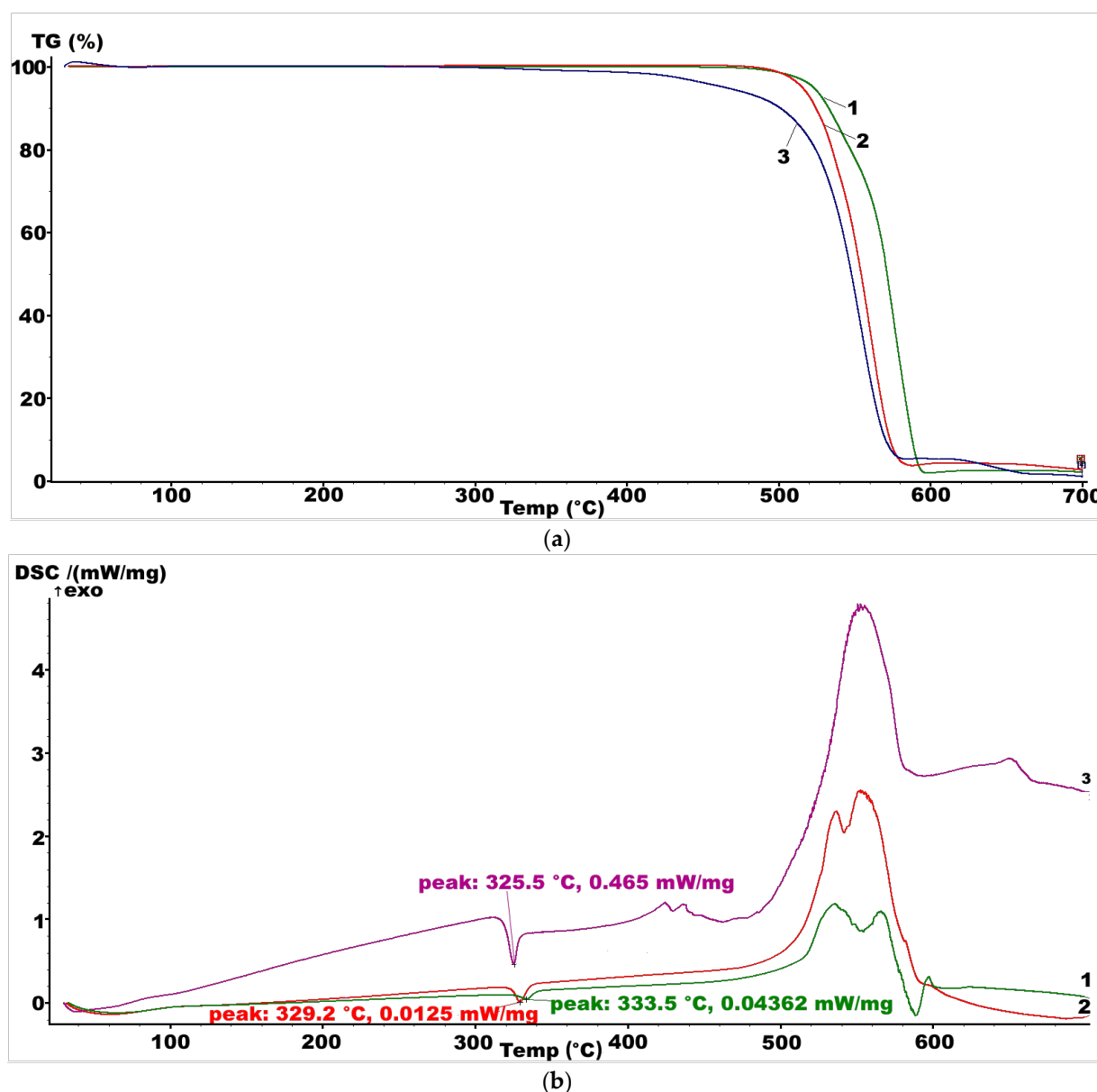


Figure 5. TG (a) and DSC (b) curves: 1—WPTFE; 2—r-PTFE; 3—TOMFLONTM.

Figure 5 shows the TG and DSC curves of fluoropolymers. The temperature of the beginning of mass loss of waste PTFE (WPTFE) is 533 °C; recycled polytetrafluoroethylene (r-PTFE)—525 °C; TOMFLONTM—501 °C (Figure 5a). Table 4 presents the temperatures at which mass loss of 10, 30, and 50 wt.% occur for WPTFE, r-PTFE, and TOMFLONTM fillers. The heat resistance of r-PTFE and TOMFLONTM powder is lower in comparison with the heat resistance of WPTFE, by 1.5% and 6.0%, respectively. The peak phase transition (melting) for WPTFE is observed at 333.5 °C and shifts to the low-temperature region for recycled fluoropolymers (r-PTFE—329.2 °C and TOMFLONTM—325.5 °C) (Figure 5b). The radiation method for producing dispersed particles is based on the low resistance of PTFE to ionizing radiation. The destruction of PTFE occurs due to the rupture of macromolecules under the influence of a flow of electrons or γ -quanta, which leads to a decrease in molecular weight by approximately 10–30 times [37]. A partial mechanical destruction of the polymer

is possible with the mechanical grinding of PTFE waste, which is also accompanied by a slight decrease in molecular weight and, as a consequence, a decrease in heat resistance and melting point (Figure 5).

Table 4. Temperatures T0.1, T0.3, and T0.5, at which, mass loss of 10, 30, and 50 wt.% occur, respectively, for different PTFE fillers.

No. Sample	PTFE Filler Type	T0.1 10 wt.%	T0.3 30 wt.%	T0.5 50 wt.%
1	WPTFE	533	559	571
2	r-PTFE	525	543	554
3	TOMFLON™	501	535	548

SEM micrographs of the cleavage surface of the elastomeric composite URC/PhFR/r-PTFE and URC/PhFR/TOMFLON™ are shown in Figures 6 and 7. A heterogeneous microstructure with a pronounced phase boundary is observed. The 10% additive results in a microstructure with well-dispersed PTFE particles in the form of spherical particles for the URC/PhFR/TOMFLON™ composite and in the form of elongated particles for the URC/PhFR/r-PTFE composite (Figure 6a,b). The elemental composition of the composite materials URC/PhFR/TOMFLON™ and URC/PhFR/r-PTFE is presented in tables in Figures 6 and 7. Two morphological phases can be distinguished in the microimages of the samples. The first composition in spectrum 1 corresponds to the antifriction filler, while the second phase in spectrum 2 characterizes the polymer–polymer mixture based on URC/PhFR (Figure 6a). The appearance of fluorine during EDS analysis in spectrum 1 (Figure 6b), spectrum 2 (Figure 7a), and spectrum 1 (Figure 7b) also indicates the presence of recycled PTFE in the form of inclusions on the background of the monolithic part of the samples. Particles' agglomeration tendency is observed with an increase in the content of the dispersed phase to 20% on SEM images (Figure 7). The maximum fluorine content increases to 39% and 70% for the URC/PhFR/TOMFLON™ and URC/PhFR/r-PTFE composites, correspondingly.

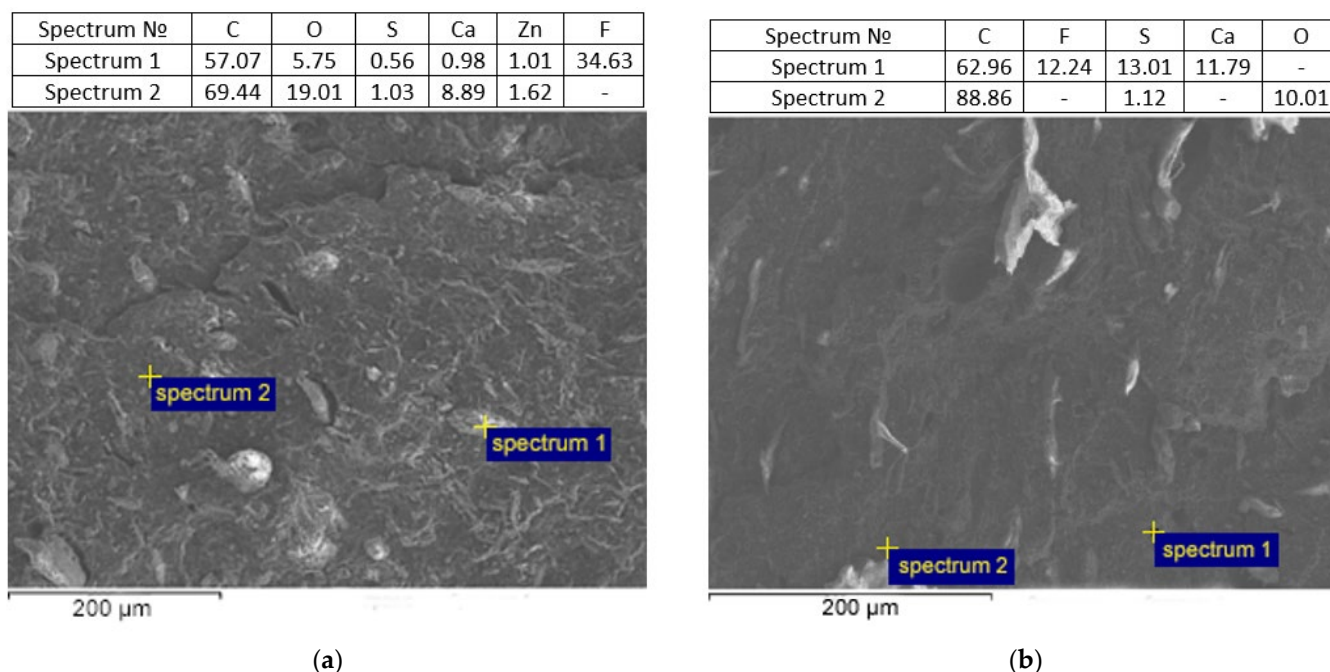


Figure 6. SEM micrographs and elemental composition of elastomeric composites with 10 wt.% PTFE content: (a) URC/PhFR/TOMFLON™; (b) URC/PhFR/r-PTFE.

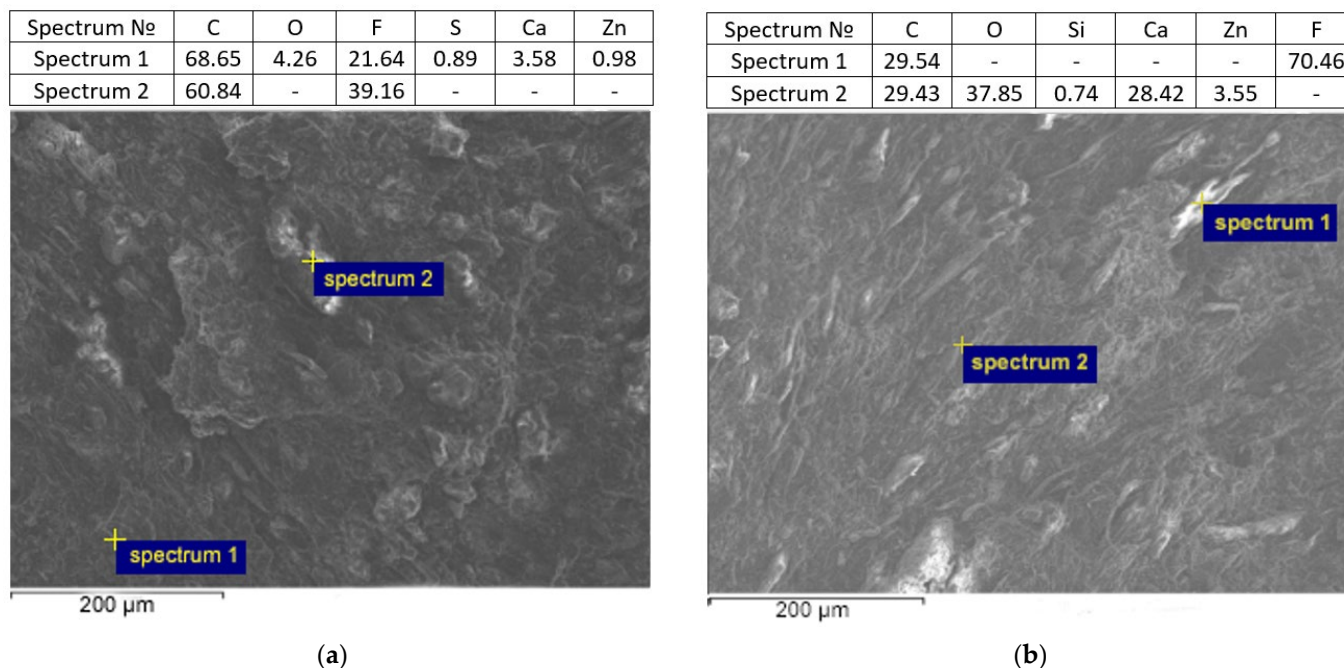


Figure 7. SEM micrographs and elemental composition of elastomeric composites with 20 wt.% PTFE content: (a) URC/PhFR/TOMFLONTM; (b) URC/PhFR/r-PTFE.

It should be also noted that a brittle fracture surface is observed for the URC/PhFR/TOMFLONTM composite, while the URC/PhFR/r-PTFE composite shows a ductile fracture surface. This difference in microstructure affects mechanical properties, which will be further discussed in this paper.

During electron irradiation, the surface of PTFE powder is functionalized with carboxylic acid fluoride (–COF) and carboxyl groups (–COOH) [25,29]. During the mechanical abrasion of WPTFE, chemical bonds in the polymer chain are broken and, as a result, active fragments of macromolecules (radicals) are formed that initiate chemical reactions with atmospheric oxygen. The presence of such functional groups and persistent reactive radicals improves the compatibility and uniform distribution of recycled PTFE in the URC/PhFR matrix. Other studies [26,37] indicate that the stimulation of intramolecular stress relaxation occurs under the influence of ionizing radiation, alternating mechanical and temperature loads. In addition, in correspondence with a decrease in polarization in PTFE particles and the transition of particles to an unpolarized equilibrium, an uncharged state takes place. This condition fosters optimizing the shape and size of the resulting ultrafine particles and, accordingly, obtaining a free-flowing PTFE powder that does not agglomerate.

On the contrary, obtaining a composite material was difficult when introducing industrial PTFE powder into the URC/PhFR elastomer matrix, which was associated with slippage and the delamination of the material during rolling.

The thermal stability of the resulting elastomeric composites was studied (Figure 8). The greatest weight loss during heat treatment at the beginning of destruction is observed for the polymer–polymer mixture URC/PhFR and the elastomeric composite URC/PhFR/TOMFLONTM, and the smallest for the elastomeric composite URC/PhFR/r-PTFE. The temperature τ_{10} at which 10% mass loss of URC/PhFR occurs is 309 °C, and for the elastomeric composites URC/PhFR/TOMFLONTM and URC/PhFR/r-PTFE, it is 316 °C and 381 °C, respectively (Table 5).

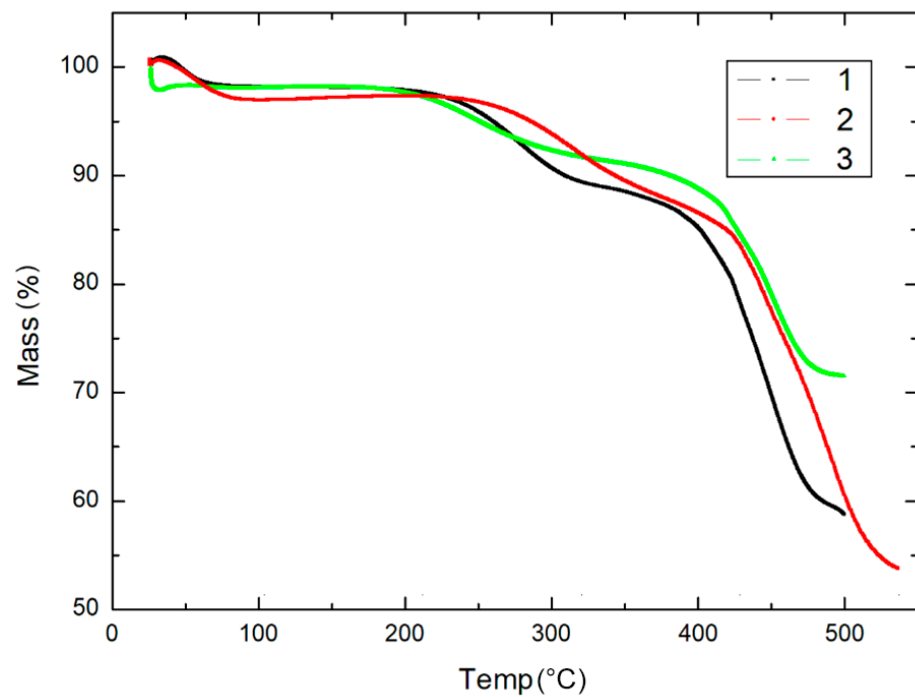


Figure 8. TG curves of polymer–polymer mixture and elastomeric composites: 1—URC/PhFR; 2—URC/PhFR/TOMFLONTM; 3—URC/PhFR/r-PTFE.

Table 5. Temperatures T0.1 and T0.3, at which, mass loss of 10 and 30 wt.% occurs, respectively, for different elastomeric composites.

No. Sample	Type of Elastomeric Composite	T0.1 10 wt.%	T0.3 30 wt.%
1	URC/PhFR	309	449
2	URC/PhFR/r-PTFE	381	499
3	URC/PhFR/TOMFLON TM	316	441

Studies of the deformation-strength properties of elastomeric composites have shown that the introduction of TOMFLONTM and r-PTFE powder leads, in general, to a decrease in strength and elongation at break, which is associated with the poor compatibility of recycled PTFE with the URC/PhPR elastomeric matrix (Figure 9). It can be seen that with a low filling of up to 10%, the deformation-strength properties of the composite are at the level of the properties of the elastomeric matrix or decrease slightly, which can be explained by the better dispersion of the filler in the matrix. With an increase in the content of antifriction filler, the agglomeration of particles is observed, which leads to an increase in internal stresses in the composite, and consequently, a decrease in deformation-strength properties.

Both PTFE fillers act as a solid lubricant for the elastomeric composites. The studies of tribological properties show that when TOMFLONTM and r-PTFE fillers are introduced into the elastomeric matrix, a decrease in the coefficient of friction (COF) (μ) is observed over the entire filling range (Figure 10).

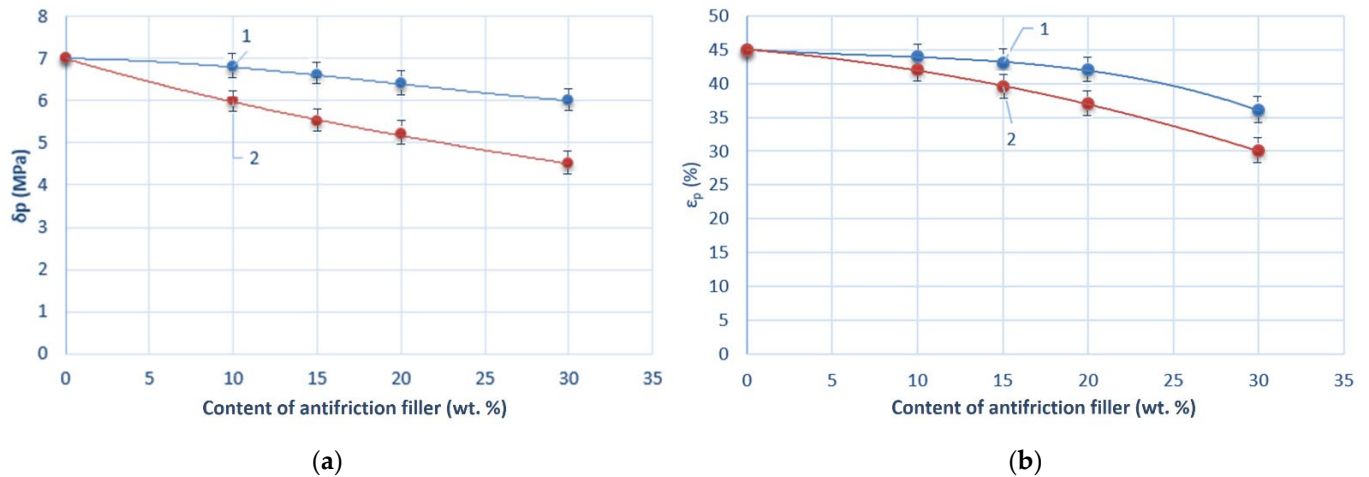


Figure 9. Deformation-strength properties of elastomeric composites 1—URC/PhFR/TOMFLONTM and 2—URC/PhFR/r-PTFE depending on the content of antifriction filler: (a) tensile strength, MPa; (b) relative elongation at break, %.

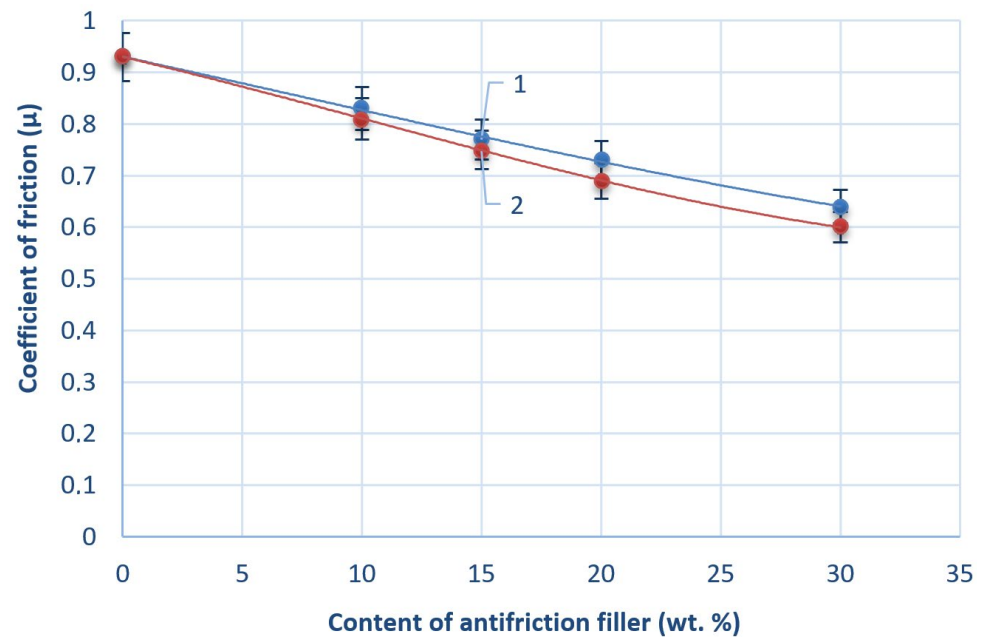


Figure 10. Coefficient of friction of an elastomeric composite depending on the content of antifriction filler: 1—URC/PhPR/r-PTFE; 2—URC/PhPR/TOMFLONTM.

A significant improvement in the tribological properties of the material is observed with the introduction of filler in an amount of 15 wt.% (Figure 11). Thus, the wear rate of materials is reduced by 20%, which is explained by the presence in the URC/PhFR elastomer matrix of a component with a low coefficient of friction and antifriction properties.

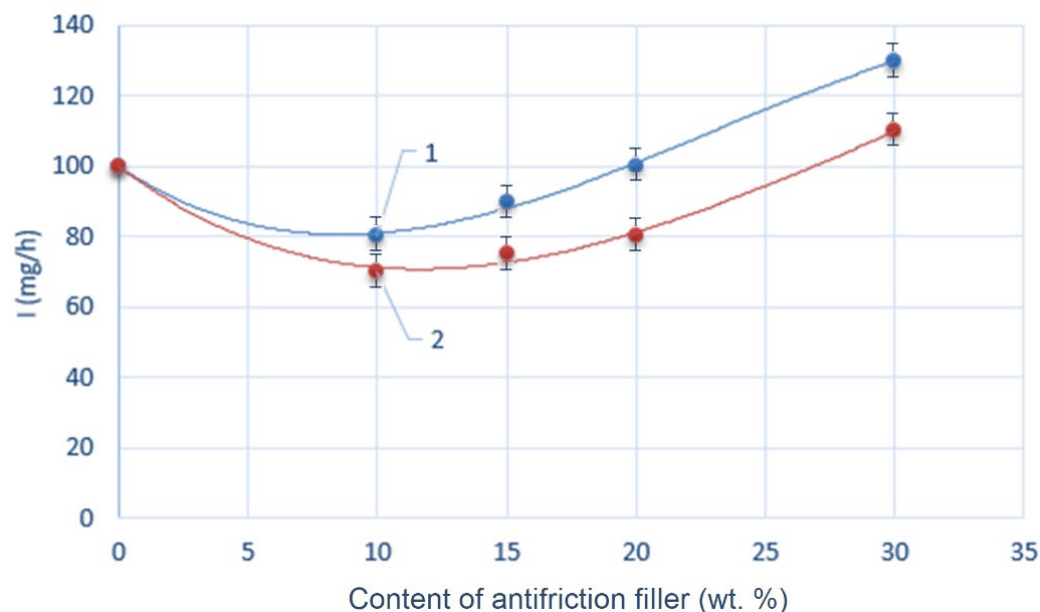


Figure 11. Wear rate of the elastomeric composite depending on the content of antifriction filler: 1—URC/PhPR/r-PTFE; 2—URC/PhPR/TOMFLON™.

4. Discussion

A comparative analysis of the deformation-strength characteristics depending on the technology for processing the antifriction filler showed that the URC/PhFR/TOMFLON™ elastomeric composite is superior to URC/PhFR/r-PTFE. According to XRD data, TOMFLON™ powder exhibits higher crystallinity of 81% (Table 3), which increases the tensile strength of the elastomeric composite. In addition, the higher dispersion of the TOMFLON™ powder, its greater functionality due to the presence of groups (–COF, –COOH), and the higher content of amorphous phase II contribute to obtaining a more homogeneous material with improved mechanical properties (tensile strength and wear resistance) due to better compatibility with the elastomeric matrix [25,29]. A mixing of the macromolecules of the initial components occurs in the boundary region between the dispersed phase of the filler and the elastomeric matrix. Apparently, in the boundary regions, shorter macromolecules of both components are mixed, the thermodynamic affinity of which is the greatest [47].

It is known that the improvement in tribological characteristics is explained by the interaction between the polymer surface, the embedded filler particles, the counter-body (often metallic), and the size of the resulting polymer wear particles [18]. The uniform distribution of r-PTFE and TOMFLON™ particles in the elastomeric matrix of URC/PhFR, due to the functional groups, leads to increased intermolecular interaction at the interface, and as a result, a decrease in the mobility of macromolecules of the components, which increases the wear resistance of the material. It is possible that friction of an elastomeric composite (with a content of up to 15 wt.% filler) is accompanied by the formation of thin, homogeneous, continuous, and durable transfer films in the form of wear products, consisting of small-sized polymer particles that act as a lubricant. It should be noted that the elastomeric composite URC/PhFR/TOMFLON™ is characterized by better wear resistance in comparison with URC/PhFR/r-PTFE. Obviously, this is due to the higher dispersion of TOMFLON™ powder, its greater functionality, and the lower molecular weight of the polymer, as was mentioned above. High content of amorphous phase II (46.9%) in TOMFLON™ powder also contributes to better friction reduction. Due to the fact that amorphous phase II is a low-molecular-weight fraction (LMWF), its macromolecules are more easily released for self-lubrication in response to applied stress and temperature [44–46]. As a result, thin transfer films may form on the opposing surface, which provide good lubrication effects and lead to increased tribological properties of the URC/PhFR/TOMFLON™ composite [48]. However, at higher filler content above 15%,

the agglomeration of its particles is observed (Figure 7), which intensifies the wear of the material (Figure 11). The presence of agglomerates and weak intermolecular interactions increase the likelihood of the formation of large wear debris. Large wear particles tend to form clumpy, discontinuous, and incomplete transfer films that are unable to produce ultra-low wear.

The enhanced performance characteristics of the developed elastomeric materials, based on industrial nitrile butadiene rubber, phenol–formaldehyde resin, and solid lubricant filler in the form of recycled PTFE, allows their use in tribological devices for the manufacture of moving seals and sliding bearings, for example, Goodrich bushings.

Previous research established that r-PTFE retains most of its mechanical properties and characteristics after processing [34]. The development of hybrid solid lubricants that combine two or more fillers with their individual advantages is a prospective area for further research and exploring new applications [49]. One possible direction is r-PTFE's combination with fullerenes and nano/micro-sized carbon particles [17]. It is necessary to point out that, depending on the application operating conditions (sliding speeds, pressure, temperature, etc.), these should be considered first while selecting additional fillers.

5. Conclusions

Elastomeric composites were obtained using waste products from polytetrafluoroethylene. A decrease in the COF of the composite material is observed after the introduction of the antifriction filler TOMFLON™ and r-PTFE. The filler content in the URC/PhFR elastomeric matrix of 15 wt.% leads to a reduction in the wear rate of the resulting materials by 20%. The results obtained show the possibility of using TOMFLON™ and r-PTFE powder in an amount of 10–15 wt.% for creating elastomeric composites with increased tribological properties.

It has been established that TOMFLON™ powder is characterized by uniform shape, homogeneous dispersion, and high content of low-molecular-weight amorphous phase II, which leads to improved tribological properties of the URC/PhFR/TOMFLON™ composite. Particles of r-PTFE powder have a greater tendency toward agglomeration and broader particle size distributions which lower the properties of the elastomeric composite. In this regard, further research is necessary to improve and modernize the PTFE waste-processing installation, which will allow an antifriction filler with improved characteristics to be obtained.

The following limitations must be taken into account in order to improve the tribological characteristics of the materials being developed, such as aggregation, the dispersion of filler particles, and functionality. Further study on the tribological performance of the PTFE elastomeric composites is necessary to have a deeper understanding of their wear mechanism. It is necessary to conduct research into contact surfaces of both components of a tribosystem, an elastomeric composite and a counterpart. In addition, the examination of wear products (debris, flake, etc.) will provide better understanding of the tribosystem components' interaction during the tests.

Author Contributions: Conceptualization, O.A. and V.K.; methodology, O.A. and V.K.; validation, V.K. and D.M.; investigation, O.A., V.K., A.D., R.K. and A.K.; data curation, O.A. and V.K.; writing—original draft preparation, O.A.; writing—review and editing, U.M.; supervision, O.A. and D.M.; project administration, D.M.; funding acquisition, V.K. and U.M. All authors have read and agreed to the published version of the manuscript.

Funding: The work was carried out within the framework of the state assignment of the Baikal Institute of Environmental Management of the Siberian Branch of the Russian Academy of Sciences (projects No. 0273-2021-0007, No. 0273-2021-0008).

Data Availability Statement: Data are contained within the article.

Acknowledgments: The work was carried out using the equipment of the Center for Collective Use of the Baikal Institute of Nature Management of the Siberian Branch of the Russian Academy of Sciences.

The authors are grateful to Kirill Demin, an engineer of the Laboratory of Physical Materials Science, Institute of Physical Materials Science SB RAS, for assistance in experiments and data visualization.

Conflicts of Interest: The authors declare no conflicts of interest.

References

1. Utrera-Barrios, S.; Araujo-Morera, J.; de Los Reyes, L.P.; Manzanares, R.V.; Verdejo, R.; López-Manchado, M.Á.; Santana, M.H. An effective and sustainable approach for achieving self-healing in nitrile rubber. *Eur. Polym. J.* **2020**, *139*, 110032. [[CrossRef](#)]
2. Shadrinov, N.; Sokolova, M.; Okhlopkova, A.; Lee, J.; Jeong, D.-Y.; Shim, E.; Cho, J.-H. Enhancement of Compatibility between Ultrahigh-Molecular-Weight Polyethylene Particles and Butadiene-Nitrile Rubber Matrix with Nanoscale Ceramic Particles and Characterization of Evolving Layer. *Bull. Korean Chem. Soc.* **2013**, *34*, 3762–3766. [[CrossRef](#)]
3. Ghosh, A.; Kannan, A.C. Nitrile rubber/peroxide treatment transformed recycled polyethylene into mechanically improved materials. *SPE Polym.* **2023**, *4*, 130–139. [[CrossRef](#)]
4. Gajdosova, V.; Strachota, B.; Strachota, A.; Michalkova, D.; Krejcikova, S.; Fulin, P.; Nyc, O.; Brinek, A.; Zemek, M.; Slouf, M. Biodegradable Thermoplastic Starch/Polycaprolactone Blends with Co-Continuous Morphology Suitable for Local Release of Antibiotics. *Materials* **2022**, *15*, 1101. [[CrossRef](#)] [[PubMed](#)]
5. Sommer, J.G. *Engineered Rubber Products*; Hanser Publishers: Munich, Germany, 2009; pp. 51–83. [[CrossRef](#)]
6. Roy, K.; Debnath, S.C.; Pongwisuthiruchte, A.; Potiyaraj, P. Recent advances of natural fibers based green rubber composites: Properties, current status, and future perspectives. *J. Appl. Polym. Sci.* **2021**, *138*, e50866. [[CrossRef](#)]
7. Dubey, K.A.; Majji, S.; Sinha, S.K.; Bhardwaj, Y.K.; Acharya, S.; Chaudhari, C.V.; Varshney, L. Synergetic effects of radiolytically degraded PTFE microparticles and organoclay in PTFE-reinforced ethylene vinyl acetate composites. *Mater. Chem. Phys.* **2013**, *143*, 149–154. [[CrossRef](#)]
8. Timoschenko, O.A.; Multanovskaya, N.A. Development of composite materials based on polyamides and elastomers for printing machine parts. *Omsk. Sci. Bull.* **2013**, *2*, 332–335.
9. Ibrahim, A.; Dahlan, M. Thermoplastic natural rubber blends. *Prog. Polym. Sci.* **1998**, *23*, 665–706. [[CrossRef](#)]
10. Cui, Z.; Jing, Y.; Wang, L.; Liu, Y.; Du, A. Thermoplastic vulcanizates with an integration of good mechanical performance and excellent resistance to high temperature and oil based on HURC/TPEE. *Polym. Adv. Technol.* **2023**, *34*, 1143–1153. [[CrossRef](#)]
11. Asaletha, R.; Kumaran, M.G.; Sabu, T. Thermoplastic elastomers from blends of polystyrene and natural rubber: Morphology and mechanical properties. *Eur. Polym. J.* **1999**, *35*, 253–271. [[CrossRef](#)]
12. Phiri, M.M.; Phiri, M.J.; Formela, K.; Wang, S.; Hlangothi, S.P. Grafting and reactive extrusion technologies for compatibilization of ground tyre rubber composites: Compounding, properties, and applications. *J. Clean. Prod.* **2022**, *369*, 133084. [[CrossRef](#)]
13. Jayakumar, A.; Radoor, S.; Parameswaranpillai, J.; Radhakrishnan, E.K.; Nair, I.C.; Siengchin, S. 3-Elastomer-based blends. In *Elastomer Blends and Composites*; Rangappa, S.M., Parameswaranpillai, J., Siengchin, S., Ozbakkaloglu, T., Eds.; Elsevier: Amsterdam, The Netherlands, 2022; pp. 33–43. [[CrossRef](#)]
14. Seema, A.; Kutty, S.K.N. Effect of an epoxy-based bonding agent on the cure characteristics and mechanical properties of short-nylon-fiber-reinforced acrylonitrile–butadiene rubber composites. *J. Appl. Polym. Sci.* **2006**, *99*, 532–539. [[CrossRef](#)]
15. Zhang, B.; Gu, B.; Yu, X. Failure behavior of resorcinol–formaldehyde latex coated aramid short-fiber-reinforced rubber sealing under transverse tension. *J. Appl. Polym. Sci.* **2014**, *132*, 41672. [[CrossRef](#)]
16. Kornopoltsev, V.N.; Mogonov, D.M.; Ayurova, O.Z.; Il'ina, O.V.; Dashitsyrenova, M.S. Reduction of negative environmental impact of mechanisms by improving tribotechnical indicators of sealing materials. *IOP Conf. Ser. Earth Environ. Sci.* **2019**, *320*, 012037. [[CrossRef](#)]
17. Lin, Z.; Zhang, K.; Ye, J.; Li, X.; Zhao, X.; Qu, T.; Liu, Q.; Gao, B. The effects of filler type on the friction and wear performance of PEEK and PTFE composites under hybrid wear conditions. *Wear* **2022**, *490–491*, 204178. [[CrossRef](#)]
18. Rosenkranz, A.; Costa, H.L.; Baykara, M.Z.; Martini, A. Synergetic effects of surface texturing and solid lubricants to tailor friction and wear—A review. *Tribol. Int.* **2021**, *155*, 106792. [[CrossRef](#)]
19. Singh, N.; Sinha, S.K. Tribological and mechanical analysis of hybrid epoxy based polymer composites with different in situ liquid lubricants (silicone oil, PAO and SN150 base oil). *Wear* **2022**, *504–505*, 204404. [[CrossRef](#)]
20. Li, D.-X.; You, Y.-L.; Deng, X.; Li, W.-J.; Xie, Y. Tribological properties of solid lubricants filled glass fiber reinforced polyamide 6 composites. *Mater. Des. (1980–2015)* **2013**, *46*, 809–815. [[CrossRef](#)]
21. Harshavardhan, B.; Ravishankar, R.; Suresha, B.; Srinivas, S.; Arun, U.; Dixit, C. Thermal characterization of polyethersulfone composites filled with self lubricants. *Mater. Today Proc.* **2021**, *43 Pt 2*, 1258–1267. [[CrossRef](#)]
22. Park, E.-S. Processibility and mechanical properties of micronized polytetrafluoroethylene reinforced silicone rubber composites. *J. Appl. Polym. Sci.* **2008**, *107*, 372–381. [[CrossRef](#)]
23. Sohail Khan, M.; Lehmann, D.; Heinrich, G. Newly developed chloroprene rubber composites based on electron-modified polytetrafluoroethylene powder. *Acta Mater.* **2009**, *57*, 4882–4890. [[CrossRef](#)]
24. Khan, M.S.; Heinrich, G. PTFE-Based Rubber Composites for Tribological Applications. In *Advanced Rubber Composites. Advances in Polymer Science*; Heinrich, G., Ed.; Springer: Berlin/Heidelberg, Germany, 2010; Volume 239, pp. 249–310. [[CrossRef](#)]
25. Cheng, S.; Kerluke, D.R. Radiation processing for modification of polymers. In Proceedings of the ANTEC 2003, Nashville, TN, USA, 4–8 May 2003; pp. 2694–2699.

26. Cao, C.; Liu, L.; Li, Q.; Chen, P.; Qian, Q.; Chen, Q. Recycling and application of wasted polytetrafluoroethylene via high-energy ball milling technology for nitrile rubber composites preparation. *Polym. Eng. Sci.* **2016**, *56*, 643–649. [[CrossRef](#)]
27. Yassien, K.M.; El-Zahhar, A.A. Investigation on the properties of gamma irradiated of polytetrafluoroethylene fibers. *Microsc. Res. Tech.* **2019**, *82*, 2054–2060. [[CrossRef](#)] [[PubMed](#)]
28. Chai, L.; Ning, K.; Qiao, L.; Wang, P.; Weng, L. Comparative study on microstructure, mechanical, and tribological property of gamma-irradiated polytetrafluoroethylene, polyetheretherketone, and polyimide polymers. *Surf. Interface Anal.* **2022**, *54*, 13–24. [[CrossRef](#)]
29. Lunkwitz, K.; Lappan, U.; Scheler, U. Modification of perfluorinated polymers by high-energy irradiation. *J. Fluor. Chem.* **2004**, *125*, 863–873. [[CrossRef](#)]
30. Kamga, L.S.; Nguyen, T.D.; Emrich, S.; Oehler, M.; Schmidt, T.; Gedan-Smolka, M.; Kopnarski, M.; Sauer, B. The effect of irradiated PTFE on the friction and wear behavior of chemically bonded PA46-PTFE-cb and PA66-PTFE-cb compounds. *Wear* **2022**, *502–503*, 204380. [[CrossRef](#)]
31. Portnyagina, V.V.; Petrova, N.N.; Mukhin, V.V.; Morozov, A.V. Chapter 12—Elastomeric composites based on propylene oxide rubber and ultrafine polytetrafluoroethylene for operation in cold climates. In *Progress in Fluorine Science, Fascinating Fluoropolymers and Their Applications*; Ameduri, B., Fomin, S., Eds.; Elsevier: Amsterdam, The Netherlands, 2020; pp. 425–462. [[CrossRef](#)]
32. Hamad, K.; Kaseem, M.; Deri, F. Recycling of waste from polymer materials: An overview of the recent works. *Polym. Degrad. Stab.* **2013**, *98*, 2801–2812. [[CrossRef](#)]
33. Darko, C.; Yung, P.W.S.; Chen, A.; Acquaye, A. Review and recommendations for sustainable pathways of recycling commodity plastic waste across different economic regions. *Resour. Environ. Sustain.* **2023**, *14*, 100134. [[CrossRef](#)]
34. Kornopol'tsev, V.N.; Ayurova, O.Z.; Dashitsyrenova, M.S.; Il'ina, O.V.; Mognonov, D.M. Preparation, Study, and Use of Composites Based on Fluoropolymer Waste. *Russ. J. Appl. Chem.* **2021**, *94*, 873–878. [[CrossRef](#)]
35. Saravanakumaar, A.; Senthilkumar, A.; Muthu Chozha Rajan, B. Effect of Fillers on Natural Fiber–Polymer Composite: An Overview of Physical and Mechanical Properties. In *Mechanical and Dynamic Properties of Biocomposites*; Krishnasamy, S., Nagarajan, R., Thiagamani, S.M.K., Siengchin, S., Eds.; WILEY-VCH: Weinheim, Germany, 2021. [[CrossRef](#)]
36. Arzhakova, O.V.; Arzhakov, M.S.; Badamshina, E.R.; Bryuzgina, E.B.; Bryuzgin, E.V.; Bystrova, A.V.; Vaganov, G.V.; Vasilevskaya, V.V.; Vdovichenko, A.Y.; Gallyamov, M.O.; et al. Polymers for the future. *Russ. Chem. Rev.* **2022**, *91*, RCR5062. [[CrossRef](#)]
37. Ignatieva, L.; Kuryavii, V.; Tsvetnikov, A.; Polyshchuk, S.; Bouznic, V. The structures of new forms of polytetrafluoroethylene obtained by modification of commercial PTFE using different methods. *J. Phys. Chem. Solids* **2007**, *68*, 1106–1111. [[CrossRef](#)]
38. Gryaznov, I.V.; Figovsky, O.L. The new technology for manufacturing polymer Nanopowder. Part 1. *Nanotechnol. Constr. A Sci. Internet-J.* **2015**, *7*, 20–45. [[CrossRef](#)]
39. GOST No. 18694-80; Standard Specifications for Hard Phenolformaldehyde Resins. Available online: <https://docs.cntd.ru/document/1200020687> (accessed on 22 December 2023). (In Russian)
40. Bruker AXS. Bruker AXS TOPAS V4: General profile and structure analysis software for powder diffraction data. In *User's Manual*; Bruker AXS: Karlsruhe, Germany, 2008.
41. Chizhov, P.; Levin, E.; Mityaev, A.; Timofeev, A. *Devices and Methods of X-ray and Electron Diffraction*; MIPT Publishing House: Moscow, Russia, 2011; pp. 1–152.
42. Bruker AXS. Bruker AXS TOPAS V4: General profile and structure analysis software for powder diffraction data. In *Technical Reference*; Bruker AXS: Karlsruhe, Germany, 2008.
43. GOST No. 11262-80; Standard Specifications for Plastics. Tensile Test Method. Available online: <https://docs.cntd.ru/document/1200004876> (accessed on 22 December 2023). (In Russian)
44. Lebedev, Y.A.; Korolev, Y.M.; Rebrov, A.V.; Ignatieva, L.N.; Antipov, E.M. X-ray diffraction phase analysis of the crystalline phase of polytetrafluoroethylene. *Crystallography* **2010**, *55*, 615–620. [[CrossRef](#)]
45. Negrov, D.A.; Eremin, E.N. Structuring Peculiarities of Polytetrafluoroethylene Modified with Boron Nitride When Activated with Ultrasonic Exposure. *Procedia Eng.* **2016**, *152*, 570–575. [[CrossRef](#)]
46. Kiryukhin, D.; Kichigina, G.; Bouznic, V. Tetrafluoroethylene telomers: Radiation-initiated chemical synthesis, properties, and application prospects. *Polym. Sci. Ser. A* **2013**, *55*, 631–642. [[CrossRef](#)]
47. Taguet, A.; Cassagnau, P.; Lopez-Cuesta, J.-M. Structuration, selective dispersion and compatibilizing effect of (nano)fillers in polymer blends. *Prog. Polym. Sci.* **2014**, *39*, 1526–1563. [[CrossRef](#)]
48. Niu, X.; Zhou, S.; Pan, D.; Zhao, Y.; Li, L. Insight into the role of debris in the formation of polytetrafluoroethylene film via molecular dynamic simulation of debris adhesion. *Polym. Eng. Sci.* **2022**, *62*, 3672. [[CrossRef](#)]
49. Praveenkumara, J.; Madhu, P.; Yashas Gowda, T.G.; Sanjay, M.R.; Siengchin, S. A Comprehensive Review on the Effect of Synthetic Filler Materials on Fiber-Reinforced Hybrid Polymer Composites. *J. Text. Inst.* **2022**, *113*, 1231–1239. [[CrossRef](#)]

Disclaimer/Publisher's Note: The statements, opinions and data contained in all publications are solely those of the individual author(s) and contributor(s) and not of MDPI and/or the editor(s). MDPI and/or the editor(s) disclaim responsibility for any injury to people or property resulting from any ideas, methods, instructions or products referred to in the content.